



HAL
open science

The Mercury Isotopic Composition of Earth's Mantle and the Use of Mass Independently Fractionated Hg to Test for Recycled Crust

Frederic Moynier, Matthew G Jackson, Ke Zhang, Hongming Cai, Saemundur Ari Halldórsson, Raphael Pik, James M D Day, Jiubin Chen

► **To cite this version:**

Frederic Moynier, Matthew G Jackson, Ke Zhang, Hongming Cai, Saemundur Ari Halldórsson, et al.. The Mercury Isotopic Composition of Earth's Mantle and the Use of Mass Independently Fractionated Hg to Test for Recycled Crust. *Geophysical Research Letters*, In press, 10.1029/2021GL094301 . hal-03321622

HAL Id: hal-03321622

<https://hal.science/hal-03321622>

Submitted on 17 Aug 2021

HAL is a multi-disciplinary open access archive for the deposit and dissemination of scientific research documents, whether they are published or not. The documents may come from teaching and research institutions in France or abroad, or from public or private research centers.

L'archive ouverte pluridisciplinaire **HAL**, est destinée au dépôt et à la diffusion de documents scientifiques de niveau recherche, publiés ou non, émanant des établissements d'enseignement et de recherche français ou étrangers, des laboratoires publics ou privés.

1 **The Mercury Isotopic Composition of Earth's Mantle and the Use of Mass**
2 **Independently Fractionated Hg to Test for Recycled Crust**

3 **Frédéric Moynier^{1,2*}, Matthew G. Jackson³, Ke Zhang⁴, Hongming Cai⁴, Sæmundur Ari**
4 **Halldórsson⁵, Raphael Pik⁶, James M.D. Day⁷, Jiubin Chen^{2,4*}**

5 ¹Université de Paris, Institut de Physique du Globe de Paris, CNRS, 1 rue Jussieu, Paris 75005, France

6 ²State Key Laboratory of Geological Processes and Mineral Resources, School of Earth Sciences, China University
7 of Geosciences, Wuhan 430074, China

8 ³Department of Earth Science, University of California, Santa Barbara, CA 93106

9 ⁴Institute of Surface-Earth System Science, Tianjin University

10 ⁵Nordic Volcanological Center, Institute of Earth Sciences, University of Iceland, Reykjavík, Iceland.

11 ⁶Centre de Recherche Pétrographique et Géochimique, CNRS, Université de Lorraine, Nancy.

12 ⁷Scripps Institution of Oceanography, University of California San Diego, La Jolla, CA 92093-0244, USA

13
14 *Corresponding authors:

15 Corresponding authors: Frederic Moynier (moynier@ipgp.fr) and Jiubin Chen
16 (jbchen@tju.edu.cn)

17 **Key Points:**

- 18 • The Hg isotopic composition of the primitive mantle determined by analysing lavas from
19 the Samoa and Iceland hotspots
20 • Key samples from the canonical mantle endmember analyzed to track crustal recycling in
21 the mantle.
22 • We demonstrate the presence of recycled oceanic and continental materials in the source
23 of ocean island basalts.

24

25

26 **Abstract**

27 **The element mercury (Hg) can develop large mass-independent fractionation (MIF) ($\Delta^{199}\text{Hg}$)**
28 **due to photo-chemical reactions at Earth's surface. This results in globally negative $\Delta^{199}\text{Hg}$**
29 **for terrestrial sub-aerially-derived materials and positive $\Delta^{199}\text{Hg}$ for sub-aqueously-derived**
30 **marine sediments. The mantle composition least affected by crustal recycling is estimated**
31 **from high- $^3\text{He}/^4\text{He}$ lavas from Samoa and Iceland, providing an average of**
32 **$\Delta^{199}\text{Hg}=0.00\pm 0.10$, $\Delta^{201}\text{Hg}=-0.02\pm 0.09$, $\delta^{202}\text{Hg}=-1.7\pm 1.2$; 2SD, N=11. By comparison, a**
33 **HIMU-type lava from Tubuai exhibits positive $\Delta^{199}\text{Hg}$, consistent with altered oceanic crust**
34 **in its mantle source. A Samoan (EM2) lava has negative $\Delta^{199}\text{Hg}$ reflecting incorporation of**
35 **continental crust materials into its source. Three Pitcairn lavas exhibit positive $\Delta^{199}\text{Hg}$ which**
36 **correlate with $^{87}\text{Sr}/^{86}\text{Sr}$, consistent with variable proportions of continental (low $\Delta^{199}\text{Hg}$ and**
37 **high $^{87}\text{Sr}/^{86}\text{Sr}$) and oceanic (high $\Delta^{199}\text{Hg}$ and low $^{87}\text{Sr}/^{86}\text{Sr}$) crustal material in their mantle**
38 **sources. These observations indicate that MIF signatures offer a powerful tool for examining**
39 **atmosphere-deep Earth interactions.**

40

41 **Plain language summary:**

42 **While Earth's mantle is continuously chemically and isotopically stirred by convection, some**
43 **ocean island lavas preserve isotopic anomalies. Their most likely origin is the recycling of**
44 **crustal material into Earth's mantle by subduction. A question is then whether these crustal**
45 **materials originate from the ocean or the continents. By using mercury stable isotopic**
46 **compositions, which have specific signatures in ocean and continent materials, we identify**
47 **whether these anomalies are due to continental or oceanic crustal material in various ocean**
48 **island basalts.**

49

50 1 Introduction

51 The composition of Earth's mantle is in part known through the chemical and isotopic analyses
52 of lavas from different tectonic settings such as mid-ocean ridge basalts (MORB) and ocean
53 island basalts (OIB) [e.g. Hofmann, 2013]. The variable isotopic compositions of OIB are
54 usually interpreted to reflect mantle heterogeneity formed by recycling of surface material back
55 into the mantle through subduction, the contribution of Earth's core into the deep source of
56 certain lavas, or the survival of early-formed heterogeneities in the mantle [e.g. Hauri and Hart,
57 1993; Hofmann, 1997; Hofmann and White, 1982; Mukhopadhyay and Parai, 2019; Mundl-
58 Petermeier et al., 2020; Rizo et al., 2019]. Identifying the geological origin of such mantle
59 sources is paramount to understand mantle dynamics through time.

60 Mantle heterogeneities have been defined and traditionally traced by using radiogenic isotopes
61 such as Sr, Nd, Hf and Pb [e.g. Blichert-Toft et al., 1999; Blichert-Toft et al., 2003; Chauvel et
62 al., 1992; Hofmann, 1988; 1997; White and Hofmann, 1982; Zindler and Hart, 1986], and
63 several end-members have been defined : EM-1 (Enriched-Mantle 1, intermediate $^{87}\text{Sr}/^{86}\text{Sr}$ and
64 low $^{206}\text{Pb}/^{204}\text{Pb}$), EM-2 (Enriched-Mantle 2, high $^{87}\text{Sr}/^{86}\text{Sr}$ and intermediate $^{206}\text{Pb}/^{204}\text{Pb}$), and
65 HIMU (defined by low $^{87}\text{Sr}/^{86}\text{Sr}$ and high $^{206}\text{Pb}/^{204}\text{Pb}$). There is a general consensus emerging for
66 the origin of EM-2 from continental crust materials (e.g. Jackson et al., 2007; White and
67 Hofmann, 1982) and HIMU as oceanic crust and lithosphere or marine carbonates (e.g. Cabral et
68 al., 2013; Chauvel et al., 1992; Hofmann and White, 1982), but the origin of EM-1 is debated
69 (e.g. continental crust, pelagic sediments, delaminated sub-continental lithosphere or a common
70 origin with EM-2 as terrestrial sediments; Castillo, 2017; Delavault et al., 2016; Eisele et al.,
71 2012; Garapic et al., 2015) and understanding its origin represents an important challenge. Stable

72 isotope systems can give complementary information to radiogenic systems, but the potential
73 sources of isotopic fractionation are diverse (e.g. magmatic differentiation, surficial processes),
74 and their interpretation can be somewhat ambiguous.

75 A few stable isotope systems, the most notable being S, O and Hg, exhibit mass-independent
76 isotopic fractionations (MIF) in naturally-occurring mantle-derived samples that are not strongly
77 modified by high temperature processes [e.g. Cabral et al., 2013; Delavault et al., 2016; Moynier
78 et al., 2020]. For example, the presence of MIF sulfur in Mangaia (Cook Islands, Polynesia) and
79 Pitcairn lavas demonstrated the presence of an Archean atmosphere-derived sulfur component in
80 their mantle source [Cabral et al., 2013; Delavault et al., 2016]. Mercury is the most volatile
81 among the moderately volatile elements [Lodders, 2013] and exhibits large mass-dependent
82 isotopic fractionations (MDF) and MIF. The MIF-Hg signatures of odd isotopes (odd-MIF) are
83 due to magnetic isotope effects [e.g. Bergquist and Blum, 2007], or a nuclear field shift effect
84 [Estrade et al., 2009] in surficial environments [e.g. Bergquist and Blum, 2007; Blum et al.,
85 2013; Chen et al., 2012; Estrade et al., 2010; Foucher and Hintelmann, 2006; Sherman et al.,
86 2010; Sonke et al., 2010], producing $> \text{‰}$ effects. High temperature processes such as magmatic
87 degassing produce limited ($< 10\text{ppm}$) Hg-MIF [Moynier et al., 2020].

88 Mercury isotopes are mass-independently fractionated in surface samples and exhibit specific
89 signatures related to different environments, showing potential application to study the nature of
90 recycled materials in the mantle sources of lavas. This is due to the distinct MIF signatures of
91 terrestrial surface environments whereby sub-aerially formed terrestrial reservoirs having
92 generally negative odd-isotopes MIF [e.g. Blum et al., 2014] while the oceanic environment,
93 including sediments and seawater, shows positive odd-isotope MIF [Meng et al., 2020; Meng et
94 al., 2019; Yin et al., 2015]. In particular, it may be possible to test whether EM1 lavas sample a

95 component of deeply recycled terrestrial sediments [Castillo, 2017; Eisele et al., 2012; Garapic et
96 al., 2015].

97 A recent landmark study showed that Hg from gold deposits associated with arc magmatism had
98 positive odd-isotope MIF associated with recycling of marine Hg from the subduction zone into
99 the mantle source of arc lavas [Deng et al., 2020]. This highlights the utility for Hg isotopes to
100 serve as a tracer of deep recycling processes, from subduction zones to hotspots. Here, we test
101 the origin of the material present in various end-member signatures (EM1, EM2, and HIMU) of
102 OIB using Hg isotopes.

103 Due to the high volatility of mercury, constraints on its isotopic composition within Earth's
104 mantle are critical for evaluating the origin of terrestrial volatile elements by means of
105 comparison with the isotopic composition of primitive meteorites [Meier et al., 2016; Moynier et
106 al., 2020]. However, the Hg isotopic composition of the mantle has been estimated from only
107 four basaltic rocks [Geng et al., 2018; Moynier et al., 2020], and these samples may not be
108 ideally suited for evaluating the composition of the primitive mantle. A primary hurdle for Hg
109 isotopic characterization of mantle-derived lavas is their low Hg contents (a few ppb). We have
110 recently developed a method that yields high precision data on less than 5ng of Hg, which
111 enables isotope characterization with just a few grams of material [Moynier et al., 2020]. This
112 allows targeting of a key set of mantle-derived lavas to evaluate the Hg isotopic composition of
113 the mantle least impacted by crustal recycling, and place key constraints on the origin of the
114 volatile element Hg on Earth.

115 To evaluate the Hg isotopic composition of the mantle least affected by crustal recycling, we
116 selected lavas with least degassed signatures reflected by their high- $^3\text{He}/^4\text{He}$ (>13 atmospheric

117 ratio, R_A), including four samples from Samoa [Jackson et al., 2007], and seven from Iceland
118 [Füri et al. 2010 and Halldórsson et al. 2016b]. To further characterize the composition of the
119 mantle we analysed three additional Icelandic samples [Óskarsson et al. 1982] and six basalts
120 from the Afar (Ethiopia) [Deng et al., 2018; Pik et al., 2006]. To search for deep recycling of
121 surface-derived Hg, samples from the three canonical mantle endmembers thought to reflect
122 deep recycling of crustal materials: EM1 (Pitcairn, N=3), HIMU (Tubuai, N=1), EM2 (Samoa,
123 N=1) were selected.

124 **2 Materials and Methods**

125 **2.1 Sample descriptions**

126 We report isotopic data on international rock standards to assess data quality and intra-laboratory
127 data comparisons: USGS samples: BCR-2 (basalt, USA), RGM-2 (Rhyolite, USA) and STM-2
128 (syenite, USA) and three Icelandic samples used as internal standards at the University of
129 Iceland (I-ICE, A-ALK, B-ALK, Óskarsson et al. 1982), all of which are available upon request.
130 The Hg isotopic composition of BCR-2 has been reported previously [Geng et al., 2018]. One
131 trachyandesite from the Samoa hotspot (ALIA-115-21) [Adams et al., 2021], three basalt
132 samples from Pitcairn [Garapic et al., 2015], and one basalt sample from Tubuai [Hauri and Hart,
133 1993] were selected to represent the EM2, EM1 and HIMU mantle end-members, respectively.
134 Four samples from Ofu island (Samoa [Jackson et al., 2007]) and seven samples from several
135 different regions (Eastern Rift Zone, Reykjanes Peninsula, Western Rift Zone, and Northern Rift
136 Zone) of Iceland [Halldórsson et al., 2016ab; Jackson et al., 2020; Macpherson et al., 2005;
137 Rasmussen et al., 2019] were taken to represent the high- $^3\text{He}/^4\text{He}$ mantle ($>13R_A$). Six basalt
138 samples from the Stratoid Series in the Afar hotspot [Deng et al., 2018; Pik et al., 2006] were

139 selected to further estimate the mantle composition. While the $^3\text{He}/^4\text{He}$ of the Afar samples have
140 not been characterized, the composition of samples from this region is $\sim 10\text{-}13 R_A$ [Marty et al.,
141 1996; Medynsky et al., 2013]. The UM-Almedén cinnabar standard was also analysed for inter-
142 laboratory comparison.

143 **2.2 Methods**

144 The method follows the same protocol as in Moynier et al. [2020]. The Hg isotopic analysis was
145 carried out using a MC-ICP-MS (Nu-Plasma-3D, Nu-Instruments) [Chen et al., 2010; Huang et
146 al., 2015; Yuan et al., 2018; Zhang et al., 2020]. The instrumental mass bias was corrected by an
147 internal NIST-SRM-997-Tl standard using the standard-sample bracketing method. All samples
148 were analyzed in three blocks (33 cycles). A 10-minute washout time in between samples

149 ensured blank levels <0.2% of the preceding sample signals. Signal intensities were 2.5V on
 150 ^{202}Hg (1 ppb solution).

151 The data for Hg-MDF is reported as $\delta^x\text{Hg}$:

$$152 \quad \delta^x\text{Hg} (\%) = [({}^x\text{Hg}/{}^{198}\text{Hg})_{\text{sample}} / ({}^x\text{Hg}/{}^{198}\text{Hg})_{\text{NIST SRM 3133}} - 1] \times 1000 \quad (\text{Eq. 1})$$

153 where x refers to 199, 200, 201, or 202. $\delta^{202}\text{Hg}$ is used for the discussion of MDF. The MIF data
 154 are defined as the deviation of the $\delta^x\text{Hg}$ from the theoretical value based on kinetic isotopic
 155 fractionation [e.g. Blum and Johnson, 2017]:

$$156 \quad \Delta^x\text{Hg} (\%) = \delta^x\text{Hg} (\%) - \beta^x \times \delta^{202}\text{Hg} \quad (\text{Eq. 2})$$

157 where the mass dependent scaling factor β^x is 0.2520, 0.5024 and 0.7520 for ^{199}Hg , ^{200}Hg and
 158 ^{201}Hg , respectively.

159 Errors are reported as twice the standard deviation from the replicates of the same solution, and
 160 are typically 0.08‰, 0.03‰, 0.03‰, 0.05‰ for $\delta^{202}\text{Hg}$, $\Delta^{199}\text{Hg}$, $\Delta^{200}\text{Hg}$ and $\Delta^{201}\text{Hg}$,
 161 respectively. Long-term measurements of UM-Almadén Hg and CRM-GBW07405 standards
 162 give identical values for Hg isotopic composition (both MDF and MIF) to literature [Chen et al.
 163 2010; Moynier et al. 2020; Huang et al. 2019], attesting the quality of Hg isotope analysis.

164 **3 Results**

165 Isotopic data for samples are reported in Table S1 and the $\Delta^{199}\text{Hg}$ values are reported
 166 against $\delta^{202}\text{Hg}$ values in Figure 1. The isotopic composition of BCR-2 is identical within error to
 167 literature values [Geng et al., 2018].

168 The terrestrial igneous rock samples show variable $\delta^{202}\text{Hg}$ values, from -3.23 to -0.01,
169 consistent with literature data [Geng et al., 2018; Moynier et al., 2020] (Figure 1). High $^3\text{He}/^4\text{He}$
170 localities - Ofu island and Iceland- do not exhibit any MIF, and the Afar samples also lack MIF-
171 Hg signatures. By contrast, the HIMU sample from Tubuai has a positive odd-isotope-MIF
172 ($\Delta^{199}\text{Hg}=+0.23\pm 0.07$). The extreme EM2 Samoa ALIA-115-21 sample has a distinct negative odd-
173 isotope-MIF signature ($\Delta^{199}\text{Hg}=-0.14\pm 0.02$). In the Pitcairn lava suite, there is a positive
174 correlation between $^{87}\text{Sr}/^{86}\text{Sr}$ and MIF-Hg: two Pitcairn lavas with the less extreme EM1 signatures
175 have clear negative odd-isotope-MIF-Hg ($\Delta^{199}\text{Hg}$ down to -0.45 ± 0.01), while the Pitcairn sample
176 with the most extreme EM1 signature has no resolvable MIF (Figure 2). No samples exhibit even-
177 isotope-MIF signatures.

178 **4. Discussion**

179 **4.1 The isotopic composition of the primitive mantle.**

180 Before discussing the potential effects of recycling of surficial material on the Hg isotopic
181 composition of mantle sources, it is critical to establish the composition of the primitive mantle.
182 OIB with the highest $^3\text{He}/^4\text{He}$ are inferred to sample mantle sources that are least degassed [Craig
183 and Lupton, 1976; Mukhopadhyay and Parai, 2019] and the least modified by crustal recycling
184 [Jackson et al., 2020; White, 2015]. Making the assumption that these samples represent materials
185 with Hg isotopic compositions consistent with the most “pristine” mantle domain, we can then
186 establish the impact of crustal subduction and recycling on the Hg systematics of mantle-derived
187 lavas.

188 The Ofu island samples have high- $^3\text{He}/^4\text{He}$ ($22R_A$ to $34R_A$, see Table S1) [Jackson et al.,
189 2007] and are inferred to sample an ancient mantle domain [Mundl-Petermeier et al., 2020] less
190 impacted by crustal recycling than other Samoan lavas [Jackson et al., 2020]. Given that the high-

191 $^3\text{He}/^4\text{He}$ reservoir is least impacted by recycling, and the discovery that some high- $^3\text{He}/^4\text{He}$ lavas
192 preserve early-Hadean signatures identified using several different short-lived isotope systems -
193 $^{129}\text{Xe}/^{130}\text{Xe}$ [Mukhopadhyay and Parai, 2019], $^{142}\text{Nd}/^{144}\text{Nd}$ [Peters et al., 2018], and $^{182}\text{W}/^{184}\text{W}$
194 [Mundl-Petermeier et al., 2020; Rizo et al., 2019]-this mantle reservoir is most likely to preserve
195 signatures associated with terrestrial accretion. Indeed, arguments have been made that the high-
196 $^3\text{He}/^4\text{He}$ reservoir is the oldest domain that has survived in Earth's mantle [Giuliani et al., 2020;
197 Jackson et al., 2010] but alternative views exist [e.g. Mukhopadhyay and Parai, 2019]. Therefore,
198 the absence of Hg-MIF in the high- $^3\text{He}/^4\text{He}$ samples suggests that Earth's mantle accreted Hg
199 devoid of MIF, and therefore any observed MIF are the consequence of terrestrial fractionation.
200 Combining Hg isotope data from the Ofu (N=4) with Iceland samples for which $^3\text{He}/^4\text{He}$ are
201 available (N=7, all of which have $13 < ^3\text{He}/^4\text{He} < 34$), return an average Hg isotopic composition for
202 the mantle of $\Delta^{199}\text{Hg}=0.00\pm 0.10$ and $\Delta^{201}\text{Hg}=-0.02\pm 0.09$ (2SD, N=11). This represents the
203 current best estimate of the terrestrial "primitive mantle" composition. The $\delta^{202}\text{Hg}$ values are more
204 variable within these samples. Since Hg is highly volatile, degassing during magma ascent can
205 induce isotopic fractionation [e.g. Zambardi et al. 2009], and further isotopic fractionation could
206 also occur during igneous processes. Therefore, compared to MIF-Hg signatures, which should
207 not be significantly impacted by high temperature magmatic and degassing processes, the $\delta^{202}\text{Hg}$
208 values are likely more impacted by the processes leading to the formation of the basalts.
209 Nevertheless, the $\delta^{202}\text{Hg}$ of the 11 high- $^3\text{He}/^4\text{He}$ samples from Ofu island and Iceland show limited
210 variation, with an average -1.7 ± 1.2 (2SD, N=11), which compare well with a previous estimate of
211 the mantle composition based on only a few unrelated igneous rocks ($\delta^{202}\text{Hg} < -2.35$, [Moynier et
212 al., 2020], see Figure S1). Furthermore, samples from the Afar ($^3\text{He}/^4\text{He} \sim 10\text{-}13 \text{ Ra}$, [Marty et al.,

213 1996; Medynsky et al., 2013]) (N=6) have similar Hg isotopic composition within error,
214 suggesting a large-scale homogeneity of Earth's modern mantle.

215 Our estimate of the primitive mantle Hg isotopic composition falls within the range defined
216 by chondrites (Figure 3). While the large uncertainties on the Hg concentration of the Earth's
217 mantle prevent an accurate estimate the amount of terrestrial Hg that is stored into the Earth's core,
218 the present chondritic isotopic composition of the Earth's primitive mantle is an argument that late
219 accretion of chondritic material delivered the present mantle Hg (and other volatile elements) (see
220 discussion in Moynier et al. [2020]). This conclusion is consistent with observations made from
221 C, N and noble gas isotopes [Marty, 2012] and the volatile and chalcophile elements S, Se and Te
222 [Wang and Becker 2013; Varas-Reus et al. 2019].

223

224 **4.2. Evidence for Hg recycling?**

225 Considering the Hg isotopic composition of high- $^3\text{He}/^4\text{He}$ lavas defined above as representative of
226 the mantle domains the least modified by crustal recycling, we can compare our estimate for the
227 Hg isotopic composition for low- $^3\text{He}/^4\text{He}$ mantle endmembers that are suggested to host recycled
228 surface materials—EM1 Pitcairn (EM1), Samoa (EM2), and Tubuai (HIMU)—and then identify
229 Hg isotope signatures associated with recycling in the mantle sources of these lavas.

230 Three OIB samples examined in this study that represent mantle end-member
231 compositions— TBA-B3 (Tubuai HIMU), ALIA-115-21 (Samoa EM2), and two Pitcairn lavas
232 (Pit-6 and Pit-8)—show clearly resolvable odd-MIF. The correlation between $\Delta^{199}\text{Hg}$ and $\Delta^{201}\text{Hg}$
233 values with a slope of ~ 1 (Figure 4), typical of surface photochemical reactions on Hg [Bergquist
234 and Blum, 2007], suggests that the three samples share likely a similar origin for the MIF
235 signatures in surficial environments. The Hg-MIF signatures in OIB therefore provides evidence

236 for recycling of shallow geochemical reservoirs into the deep sources of hotspots. This correlation
237 between $\Delta^{199}\text{Hg}$ and $\Delta^{201}\text{Hg}$ values also provides further confidence on the quality of the data as
238 isobaric interference would produce isotopic signatures that lie outside of this range.

239 Photochemical reduction of aqueous Hg(II) to Hg(0) vapor is the major source of odd-MIF,
240 and is the main pathway of transfer of Hg from the ocean (surface) to the atmosphere [e.g.
241 Bergquist and Blum, 2007]. During the photochemical reduction, a positive $\Delta^{199}\text{Hg}$ [Hg(II)] is
242 retained in the marine environment while the complementary negative $\Delta^{199}\text{Hg}$ [Hg(0)] is released
243 into the atmosphere [e.g. Bergquist and Blum, 2007]. Given the short residence time of Hg(0) in
244 the atmosphere (~ 1 year), its quick subsequent deposition confers a globally negative $\Delta^{199}\text{Hg}$ to
245 the terrestrial reservoirs, while marine environments are characterized by positive $\Delta^{199}\text{Hg}$ [e.g.
246 Biswas et al., 2008; Blum et al., 2014; Demers et al., 2015; Grasby et al., 2017; Jiskra et al., 2017].
247 How a negative $\Delta^{199}\text{Hg}$ preserved in terrestrial material is then transported into the ocean through
248 time is unclear at present. Further work is required to test the robustness of this negative signature
249 on long timescales necessary for this material to be recycled within the mantle. This difference
250 between terrestrial and marine settings is well reflected in sediments, with generally negative
251 $\Delta^{199}\text{Hg}$ in coastal sediments (which originate via erosion of nearby terrestrial materials) and
252 positive $\Delta^{199}\text{Hg}$ for open sea marine sediments [e.g. Meng et al., 2019; Yin et al., 2015]. The odd-
253 MIF of ALIA-115-21 (Samoa EM2), TBA-B3 (Tubuai HIMU), and Pit-6 and Pit-8 (Pitcairn)
254 therefore likely reflect a marine Hg isotopic signature in Tubuai, and continental Hg signatures
255 Samoan EM2 lavas (Figure 4). As discussed below, Pitcairn lavas exhibit Hg isotopic evidence for
256 recycled marine and terrestrial materials.

257 The presence of marine and continental signatures in the mantle sources of Tubuai HIMU and
258 Samoa EM2 lavas, respectively, is consistent with traditional interpretations based on radiogenic

259 isotope signatures. Tubuai exhibits a HIMU signature, which is considered to result from recycling
260 of ancient oceanic crust into the mantle [Hofmann and White, 1982]. The geochemically-depleted
261 $^{87}\text{Sr}/^{86}\text{Sr}$ and $^{143}\text{Nd}/^{144}\text{Nd}$ signatures in HIMU lavas globally precludes a significant sediment
262 (terrigenous or marine) contribution to their mantle sources, but transfer of positive $\Delta^{199}\text{Hg}$ isotope
263 compositions of seawater to oceanic crust during hydrothermal circulation at a mid-ocean ridge
264 could explain the MIF signatures in Tubuai HIMU OIB. A potential caveat with this model is the
265 low abundance of Hg in seawater compared to fresh basalts that would require a water/rock ratio
266 of ~ 1000 to transfer the Hg isotopic composition of seawater to oceanic crust. However, the
267 absence of data on Hg behavior during seawater alteration of oceanic crust (e.g., Hg concentration
268 measurements on altered oceanic crust, including serpentinites) limits our ability to quantitatively
269 model this scenario. An additional complexity is that a fraction of the slab Hg budget would be
270 lost during subduction dehydration, but relevant data are not yet available to quantify this. By
271 contrast, Samoan EM2 lavas exhibit geochemically-enriched (high) $^{87}\text{Sr}/^{86}\text{Sr}$ and (low) $^{143}\text{Nd}/^{144}\text{Nd}$
272 signatures consistent with the input of recycled terrigenous materials [Jackson et al., 2007;
273 Workman et al., 2008], consistent with the slightly negative $\Delta^{199}\text{Hg}$ terrestrial signature.

274 The presence of negative $\Delta^{199}\text{Hg}$ in the source of Pitcairn EM1 OIB suggests that, like EM2,
275 EM1 contains a fraction of recycled terrigenous material [Castillo, 2017; Delavault et al., 2016;
276 Stracke, 2012]. However, there is complexity in the MIF present in the Pitcairn suite that is not
277 explained by our simple model: the correlation between the $\Delta^{199}\text{Hg}$ and $^{87}\text{Sr}/^{86}\text{Sr}$ for the three
278 Pitcairn samples (Figure 2) is puzzling, as we would expect the sample with the highest $^{87}\text{Sr}/^{86}\text{Sr}$
279 to host the largest fraction of continent-derived material and, therefore, the lowest $\Delta^{199}\text{Hg}$. Instead,
280 the Pitcairn lava with the weakest EM1 signature has the strongest negative $\Delta^{199}\text{Hg}$, and the most
281 extreme EM1 Pitcairn lava has no resolvable $\Delta^{199}\text{Hg}$ signature. The positive correlation between

282 $\Delta^{199}\text{Hg}$ and $^{87}\text{Sr}/^{86}\text{Sr}$ is unlikely to be explained by seawater alteration, a mechanism that would
283 increase both $\Delta^{199}\text{Hg}$ and $^{87}\text{Sr}/^{86}\text{Sr}$. This is because 1) $\Delta^{199}\text{Hg}$ also exhibit a negative correlation
284 with $^{143}\text{Nd}/^{144}\text{Nd}$ (Figure S2), a radiogenic isotope system immune to seawater influence, and 2)
285 the selected Pitcairn lavas are young ($<1.0\text{Ma}$; [Duncan et al., 1974]) and fresh (i.e., no signs of
286 visible alteration). Therefore, we explore a mantle source origin for the correlation between
287 $^{87}\text{Sr}/^{86}\text{Sr}$ and $\Delta^{199}\text{Hg}$, acknowledging that this relationship is only for three samples.

288 Unlike Samoan EM2 (which is a melt of a peridotite mantle source that hosts recycled
289 terrigenous material) [Jackson and Shirey, 2011] and Tubuai HIMU (which is a melt of a
290 mantle source with recycled oceanic crust) [Hauri and Hart, 1993], extreme Pitcairn EM1 is
291 suggested to host both recycled oceanic crust and terrigenous materials [Eisele et al., 2003]. A
292 mixture of both recycled oceanic crust and terrigenous materials can help to explain the correlation
293 between $\Delta^{199}\text{Hg}$ and $^{87}\text{Sr}/^{86}\text{Sr}$ (Figure 2), where Pitcairn's extreme EM1 endmember
294 (highest $^{87}\text{Sr}/^{86}\text{Sr}$) lacks a clear odd-MIF, and the Pitcairn lava with the weakest EM1 signature
295 (lowest $^{87}\text{Sr}/^{86}\text{Sr}$) has a negative $\Delta^{199}\text{Hg}$. Because recycled oceanic crust and terrigenous materials
296 have complementary positive and negative $\Delta^{199}\text{Hg}$ signatures, respectively, it is possible for their
297 mixture to generate in a near-zero $\Delta^{199}\text{Hg}$ value like that observed in the extreme Pitcairn EM1
298 sample. In this case, the presence of terrigenous materials explains the high $^{87}\text{Sr}/^{86}\text{Sr}$ in the extreme
299 EM1 Pitcairn lava. In contrast, the Pitcairn lava with the lowest $^{87}\text{Sr}/^{86}\text{Sr}$ (weakest EM1
300 signature) is explained by a smaller fraction of recycled terrigenous material, and the very negative
301 $\Delta^{199}\text{Hg}$ in this lava can explained by the absence (or near absence) of oceanic crust (which would
302 have a positive $\Delta^{199}\text{Hg}$ values): the remaining contribution of recycled terrigenous material has
303 strongly negative $\Delta^{199}\text{Hg}$, and explains the negative $\Delta^{199}\text{Hg}$ values determined in lavas. In this
304 way, the relative proportions and absolute abundances of recycled terrigenous and oceanic crust

305 materials can be modulated to explain the magnitude and sign of the $\Delta^{199}\text{Hg}$ values, and its
306 relationship with radiogenic isotopes.

307

308 **5. Conclusions**

309 To estimate the Hg isotopic composition of the mantle that is least affected by crustal
310 recycling, we analysed high- $^3\text{He}/^4\text{He}$ lavas from Samoa and Iceland. We obtained an average
311 $\Delta^{199}\text{Hg}=0.00\pm 0.10$, $\Delta^{201}\text{Hg}=-0.02\pm 0.09$ and $\delta^{202}\text{Hg}=-1.7\pm 1.2$ (2SD, N=11), which is the best
312 estimate for the composition of the primitive mantle.

313 HIMU lavas from Tubuai exhibit positive Hg-MIF, likely reflecting a transfer of the
314 isotope compositions of seawater to oceanic crust during hydrothermal circulation at a mid-ocean
315 ridge; positive Hg-MIF therefore signals the presence of altered oceanic crust in its mantle source.
316 The negative MIF observed for EM2 lava from Samoa is consistent with assimilation of
317 continental crust material. The negative MIF for the Pitcairn lavas, and the positive correlation of
318 $\Delta^{199}\text{Hg}$ values with $^{87}\text{Sr}/^{86}\text{Sr}$, provides an independent argument in favor of mixture between
319 terrestrial and marine materials in the mantle source of EM1.

320 **Acknowledgments, Samples, and Data**

321 Runsheng Yin and Michael Bizimis are thanked for insightful reviews that have improved this
322 manuscript. This study was supported by the National Natural Science Foundation of China
323 (41625012, 41961144028, U1612442, 41830647) to JB.C and by the China National Space
324 Administration (No. D020205) to ZW. FM thanks Yongsheng Liu for making the visit at CUG
325 Wuhan possible. MGJ thanks IGP for providing a stimulating academic home during sabbatical,
326 and acknowledges partial support from NSF EAR-1900652 and OCE-1928970.

327 **Open Research section**

328 All the data are presently provided as a supplementary table and will be deposit on the CNRS HAL
329 website as well as on the database Earthchem: <https://earthchem.org/>

330
331 **References:**

- 332 Adams, J., J. M., F. Spera, A. Price, B. Byerly, G. Seward, and J. Cottle (2021), Extreme isotopic
333 heterogeneity in Samoan clinopyroxenes constrains sediment recycling, *Nature com.*, 12, 1234.
334 Bergquist, B. A., and J. D. Blum (2007), Mass-dependent and-independent fractionation of Hg
335 isotopes by photoreduction in aquatic systems, *Science*, 318, 417-420.
336 Biswas, A., J. D. Blum, B. A. Bergquist, G. J. Keeler, and Z. Xie (2008), Natural mercury isotope
337 variation in coal deposits and organic soils, *Env. Sci. & Tech.*, 42, 8303-8309.
338 Blichert-Toft, J., F. A. Frey, and F. Albarède (1999), Hf isotope evidence for pelagic sediments in
339 the source of Hawaiian basalts, *Science*, 285, 879-882.
340 Blichert-Toft, J., D. Weis, C. Maerschalk, A. Agranier, and F. Albarède (2003), Hawaiian hot spot
341 dynamics as inferred from the Hf and Pb isotope evolution of Mauna Kea volcano, *Geochem.*
342 *Geophys. Geosyst.*, 4, doi:10.1029/2002GC000340.
343 Blum, J., and M. Johnson, W. (2017), Recent developments in mercury stable isotopes analysis,
344 in *Non-traditional stable isotopes*, edited by F.-Z. Teng, J. Watkins and N. Dauphas, pp. 733-757,
345 Mineralogical society of America.
346 Blum, J., B. Popp, J. Drazen, C. Choy, and M. Johnson (2013), Evidence for methylmercury
347 production below the mixed layer in the central North Pacific Ocean, *Nat. Geosci.*, 6, 879-884.
348 Blum, J., L. Sherman, and M. W. Johnson (2014), Mercury Isotopes in Earth and Environmental
349 Sciences, *A. Rev. Earth and Plane. Sci.*, 42, 249-269.
350 Cabral, R., M. Jackson, E. Rose-Koga, K. Koga, M. Whitehouse, M. Antonelli, J. Farquhar, J. Day,
351 and E. Hauri (2013), Anomalous sulphur isotopes in plume lavas reveal deep mantle storage of
352 Archaean crust, *Nature*, 496, 490-493.
353 Castillo, P. (2017), An alternative explanation for the Hf-Nd mantle array, *Science Bulletin*, 62,
354 974-975.
355 Chauvel, C., A. W. Hofmann, and P. Vidal (1992), HIMU-EM: The French Polynesian connection,
356 *Earth Planet. Sci. Lett.*, 110, 99-119.
357 Chen, J., H. Hintelmann, and B. Dimock (2010), Chromatographic pre-concentration of Hg from
358 dilute aqueous solutions for isotopic measurement by MC-ICP-MS, *J. Anal. Atom. Spec.*, 25,
359 1402-1409.
360 Chen, J., H. Hintelmann, X. Feng, and B. Dimock (2012), Unusual fractionation of both odd and
361 even mercury isotopes in precipitation from Peterborough, ON, Canada, *Geochim. Cosmochim.*
362 *Acta*, 90, 33-46.
363 Craig, H., and J. E. Lupton (1976), Primordial neon, helium, and hydrogen in oceanic basalts,
364 *Earth Planet. Sci. Lett.*, 31, 369-385.
365 Delavault, H., C. Chauvel, E. Thomassot, C. Devey, and B. Dazas (2016), Sulfur and lead isotopic
366 evidence of relic Archean sediments in the Pitcairn mantle plume, *Proc. Nat. Ac. Sci.*, 113,
367 12952-12956.

- 368 Demers, J. D., J. Blum, and D. Zac (2015), Mercury isotopes in a forested ecosystem:
369 Implications for air-surface exchange dynamics and the global mercury cycle., *Adv. Earth Space*
370 *Sci.* 27, 222-238.
- 371 Deng, C., G. Sun, Y. Rong, R. Sun, D. Sun, B. Lehmann, and R. S. Yin (2020), Recycling of mercury
372 from the atmosphere-ocean system into volcanic arc associated epithermal gold systems.
373 *Geology*, 49, 309–313.
- 374 Deng, Z., M. Chaussidon, P. Savage, F. Robert, R. Pik, and F. Moynier (2018), Titanium isotopes
375 as a tracer for the plume or island arc affinity of felsic rocks, *Proc. Nat. Ac. Sci.*, 116, 1132-1135.
- 376 Duncan, R., McDougall, I., Carter, R., Coombs, D., 1974. Pitcairn island— another Pacific hot
377 spot? *Nature* 251, 619–682.
- 378 Eisele, J., W. Abouchami, S. J. G. Galer, and A. W. Hofmann (2003), The 320 kyr Pb isotope
379 evolution of Mauna Kea lavas recorded in the HSDP-2 drill core, *Geochem. Geophys. Geosyst.*,
380 4, doi: 10.1029/2002GC000339.
- 381 Eisele, J., M. Sharma, S. J. G. Galer, J. Blichert-Toft, C. Devey, and A. W. Hofmann (2012), The
382 role of sediment recycling in EM-1 inferred from Os, Pb, Hf, Nd, Sr isotope and trace element
383 systematics of the Pitcairn hotspot, *Earth Planet. Sci. Lett.*, 196, 197-212.
- 384 Estrade, E., J. Carignan, J. E. Sonke, and O. Donard (2009), Mercury isotope fractionation during
385 liquid-vapor evaporation experiments, *Geochim. Cosmochim. Acta*, 73, 2693-2711.
- 386 Estrade, N., J. Carignan, and O. Donard (2010), Isotope tracing of atmospheric mercury sources
387 in an urban area of northeastern France, *Environ. Sci. Technol.*, , 44, 6062-6067.
- 388 Foucher, D., and H. Hintelmann (2006), High-precision measurement of mercury isotope ratios
389 in sediments using cold-vapor generation multi-collector inductively coupled plasma mass
390 spectrometry, *Anal. Bioanal. Chem.*, 384, 1470-1478.
- 391 Füre, E., D. Hilton, S. Halldórsson, P. Barry, D. Hahm, T. Fischer, and K. Grönvold (2010),
392 Apparent decoupling of the He and Ne isotope systematics of the Icelandic mantle: The role of
393 He depletion, melt mixing, degassing fractionation and air interaction, *Geochim. Cosmochim.*
394 *Acta*, 74, 3307–3332.
- 395 Garapic, G., M. Jackson, E. Hauri, S. R. Hart, K. A. Farley, J. Blusztajn, and J. Woodhead (2015), A
396 radiogenic isotopic (He-Sr-Nd-Pb-Os) study of lavas from the Pitcairn hotspot: Implications for
397 the origin of EM-1 (enriched mantle 1), *Lithos*, 228, 1-11.
- 398 Geng, H., R. S. Yin, and X. Li (2018), An optimized protocol for high precision measurement of
399 Hg isotopic compositions in samples with low concentrations of Hg using MC-ICP-MS, *J. Anal.*
400 *Atom. Spec*, 33, 1932-1940.
- 401 Giuliani, A., M. G. Jackson, A. Fitzpyane, and H. Dalton (2020), Remnants of early Earth
402 differentiation in the deepest mantle-derived lavas., *Proc. Nat. Ac. Sci*, 118, e2015211118.
- 403 Grasby, S. E., W. Shen, R. Yin, J. D. Gleason, J. D. Blum, and R. F. Lepak (2017), Isotopic
404 signatures of mercury contamination in latest Permian oceans, *Geology*, 45, 55-58.
- 405 Halldórsson, S., J. Barnes, A. Stefánsson, D. Hilton, E. Hauri, and E. Marshall (2016a), Subducted
406 lithosphere controls halogen enrichments in the Iceland mantle plume source, *Geology*, 44,
407 679-682.
- 408 Halldórsson, S., D. Hilton, P. Barry, E. Füre, and K. Grönvold (2016b), Recycling of crustal material
409 by the Iceland mantle plume: new evidence from nitrogen elemental and isotope systematics of
410 subglacial basalts, *Geochim. Cosmochim. Acta*, 176, 206-226.

- 411 Hauri, E. H., and S. R. Hart (1993), Re-Os isotope systematics of EMII and HIMU oceanic basalts
412 from the south Pacific Ocean, *Earth Planet. Sci. Lett.*, 114, 353-371.
- 413 Hofmann, A. W. (1988), Chemical differentiation of the Earth: the relationship between mantle
414 continental crust, and oceanic crust, *Earth Planet. Sci. Letters*, 90, 297-314.
- 415 Hofmann, A. W. (1997), Mantle geochemistry: the message from oceanic volcanism, *Nature*,
416 385, 219-229.
- 417 Hofmann, A. W. (2013), Sampling Mantle Heterogeneity through Oceanic Basalts: Isotopes and
418 Trace Elements, in *Treatise on Geochemistry*, edited by H. D. Holland and K. K. Turekian, pp. 61-
419 101, Elsevier.
- 420 Hofmann, A. W., and W. M. White (1982), Mantle plumes from ancient oceanic crust, *Earth*
421 *Planet. Sci. Lett.*, 57, 421-436.
- 422 Huang, Q., Y. Liu, J. Chen, X. Feng, W. Huang, S. Yuan, H. Cai, and X. Fu (2015), An improved
423 dual-stage protocol to pre-concentrate mercury from airborne particles for precise isotopic
424 measurement., *J. Anal. Atom. Spectr.*, 30, 957–966.
- 425 Huang, Q., Chen, J., Huang, W., Reinfelder, J.R., Fu, P., Yuan, S., Wang, Z., Yuan, W., Cai, H.,
426 Ren, H., 2019. Diel variation in mercury stable isotope ratios records photo-reduction of PM 2.5-
427 bound mercury. *Atmos. Chem. Phys.* 10, 315–325.
- 428 Jackson, M., S. R. Hart, A. Koppers, H. Staudigel, J. Konter, J. Blusztajn, M. Kurz, and J. Russell
429 (2007), The return of subducted continental crust in Samoan lavas, *Nature* 448, 684-687.
- 430 Jackson, M. G., et al. (2020), Ancient He and W isotopic signatures preserved in mantle domains
431 least modified by crustal recycling, *PNAS*, 117, 30993-31001.
- 432 Jackson, M. G., R. Carlson, M. Kurz, P. D. Kempton, D. Francis, and J. Blusztajn (2010), Evidence
433 for the survival of the oldest terrestrial mantle reservoir., *Nature*, 466, 853-856.
- 434 Jackson, M. G., and S. B. Shirey (2011), Re–Os isotope systematics in Samoan shield lavas and
435 the use of Os-isotopes in olivine phenocrysts to determine primary magmatic compositions,
436 *Earth Planet. Sci. Lett.*, 312, 91-101.
- 437 Jiskra, M., J. G. Wiederhold, U. Skjellberg, R. M. Kronberg, and R. Kretzschmar (2017), Source
438 tracing of natural organic matter bound mercury in boreal forest runoff with mercury stable
439 isotopes, *Environmental Science: Processes & Impacts*, 19, 1235-1248.
- 440 Macpherson, C. C., D. Hilton, J. Day, D. Lowry, and K. Gronvold (2005), High- $^3\text{He}/^4\text{He}$, depleted
441 mantle and low d^{18}O , recycled oceanic lithosphere in the source of central Iceland magmatism,
442 *Earth Planet. Sci. Lett.*, 233, 411–427.
- 443 Marty, B. (2012), The origins and concentrations of water, carbon, nitrogen and noble gases on
444 Earth, *Earth Planet. Sci. Lett.*, 314, 56-66.
- 445 Marty, B., R. Pik, and Y. Gezahegn (1996), Helium isotopic variations in Ethiopian plume lavas:
446 nature of magmatic sources and limit on lower mantle contribution, *Earth Planet. Sci. Lett.*, 144,
447 223-237.
- 448 Medynsky, S., et al. (2013), Control on magmatic cycles and development of rift topography of the
449 Manda Hararo segment (Afar, Ethiopia): Insights from cosmogenic ^3He
450 investigation of landscape evolution, *Earth Planet. Sci. Lett.*, 367, 133-145.
- 451 Meier, M., C. Cloquet, and B. Marty (2016), Mercury (Hg) in meteorites: Variations in
452 abundance, thermal release profile, mass-dependent and mass-independent isotopic
453 fractionation, *Geochim Cosmochim Acta*, 182, 55-72.

- 454 Meng, M., R. Sun, H. Liou, B. Yu, Y. Yin, L. Hu, J. Chen, J. Shi, and G. Jiang (2020), Mercury
455 isotope variations within the marine food web of Chinese Bohai Sea: Implications for mercury
456 sources and biogeochemical cycling, *J. of Haz. Mat.*, 384, 121379.
- 457 Meng, M., R. Y. Sun, H. W. Liu, B. Yu, Y. G. Yin, L. G. Hu, J. B. Shi, and G. B. Jiang (2019), An
458 integrated model for input and migration of mercury in Chinese coastal sediments, *Environ. Sci.*
459 *Technol.*, 53, 2460-2471.
- 460 Moynier, F., J. Chen, K. Zhang, H. Cai, Z. Wang, M. G. Jackson, and J. Day (2020), Chondritic
461 mercury isotopic composition of Earth and evidence for evaporative equilibrium degassing
462 during the formation of eucrites, *Earth Planet. Sci. Lett.*, 551, 116544.
- 463 Mukhopadhyay, S., and R. Parai (2019), Noble Gases: A Record of Earth's Evolution and Mantle
464 Dynamics, *Annual Rev. Earth Planet. Sci.*, 47, 389-419.
- 465 Mundl-Petermeier, A., R. J. Walker, R. A. Fischer, V. Lekic, M. Jackson, and M. Kurz (2020),
466 Anomalous ^{182}W in high $^3\text{He}/^4\text{He}$ ocean island basalts: fingerprints of Earth's core?, *Geochim.*
467 *Cosmochim. Acta* 194–211.
- 468 Óskarsson, N., Sigvaldason, G.E., and Steinthorsson, S., 1982, A dynamic-model of rift-zone
469 petrogenesis and the regional petrology of Iceland: *Journal of Petrology*, v. 23, p. 28–74, doi: 10
470 .1093 /petrology /23 .1 .28.
- 471 Peters, B. J., R. Carlson, J. M. D. Day, and M. F. Horan (2018), Hadean silicate differentiation
472 preserved by anomalous $^{142}\text{Nd}/^{144}\text{Nd}$ ratios in the Réunion hotspot source., 555, 89-93.
- 473 Pik, R., B. Marty, and D. Hilton (2006), How many mantle plumes in Africa? The geochemical
474 point of view, *Chem. Geol.*, 226, 100-114.
- 475 Rasmussen, M. B., S. A. Halldórsson, S. A. Gibson, and G. H. Guðfinnsson (2019), Olivine
476 chemistry reveals compositional source heterogeneities within a tilted mantle plume beneath
477 Iceland, *Earth Planet. Sci. Lett.*, 531, 116008.
- 478 Rizo, H., D. Andrault, N. Bennet, M. Humayun, A. Brandon, I. Vlastelic, B. Moine, A. Poirier, M.
479 Bouhifd, and D. Murphy (2019), ^{182}W evidence for core-mantle interaction in the source of
480 mantle plumes., *Geochem. Perspect. Lett.*, 11, 6-11.
- 481 Sherman, L., J. Blum, K. Johnson, G. Keeler, J. Barres, and T. Douglas (2010), Mass-independent
482 fractionation
483 of mercury isotopes in Arctic snow driven by sunlight, *Nat. Geosci.*, 3, 173-177.
- 484 Sonke, J., J. Schafer, J. Chmeleff, S. Audry, G. Blanc, and B. Dupre (2010), Sedimentary mercury
485 stable isotope
486 records of atmospheric and riverine pollution from two major European heavy metal refineries,
487 *Chem. Geol.*, 279, 90-100.
- 488 Stracke, A. (2012), Earth's heterogeneous mantle: A product of convection-driven interaction
489 between crust and mantle, *Chem. Geol.*, 330, 274-299.
- 490 Varas-Reus, M. I., S. König, A. Yierpan, J. P. Lorand, and R. Schoenberg (2019), Selenium
491 isotopes as tracers of a late volatile contribution to Earth from the outer Solar System, *Nature*
492 *Geosci.*, 12, 779–782.
- 493 Wang, Z. Z., and H. Becker (2013), Ratios of S, Se and Te in the silicate Earth require a volatile-
494 rich late veneer, *Nature*, 499, 328-331.
- 495 White, W. (2015), Isotopes, DUPAL, LLSVPs, and Anekantavada., *Chem. Geol.*, 419, 10–28.
- 496 White, W. M., and A. W. Hofmann (1982), Sr and Nd isotope geochemistry of oceanic basalts
497 and mantle evolution, *Nature*, 296, 821-825.

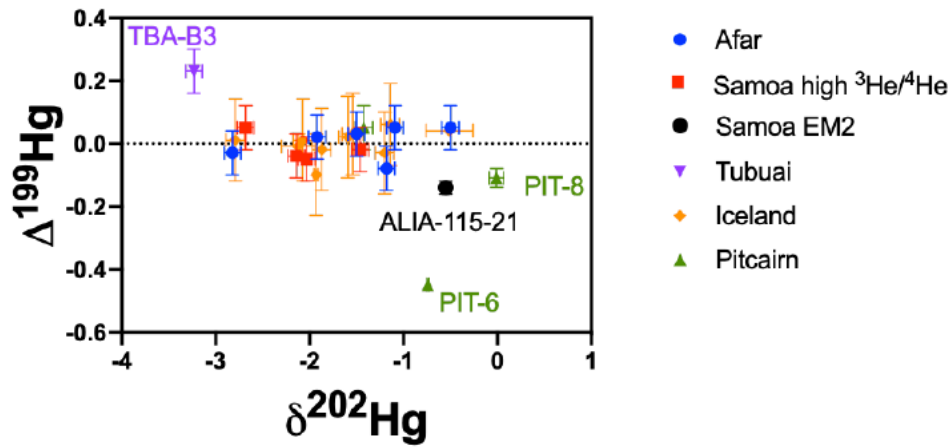
498 Workman, R. K., S. Hart, J. Eiler, and M. Jackson (2008), Oxygen isotopes in Samoan lavas:
499 confirmation of continent recycling, *Geology*, 36, 551-554.
500 Yin, R. S., X. B. Feng, B. Chen, J. Zheng, W. Wang, and X. Li (2015), Identifying the source and
501 processes of mercury in subtropical estuarine and ocean sediments using Hg isotopic
502 composition., *Environ. Sci. Tech.*, 49, 1347-1355.
503 Yuan, S., J. Chen, H. Cai, W. Yuan, Z. Wang, Q. Huang, Y. Liu, and X. Wu (2018), Sequential
504 samples reveal significant variation of mercury isotope ratios during single rainfall events., *Sci.*
505 *Total Environ.*, 624, 133-144.
506 Zambardi, T., J. Sonke, J.-P. Toutain, F. Sortnob, and H. Shinoharac (2009), Mercury emissions
507 and stable isotopic compositions at Vulcano Island (Italy), *Earth Planet. Sci. Lett.*, 277, 236-243.
508 Zhang, Y., et al. (2020), Mercury isotope compositions in large anthropogenically impacted
509 Pearl River, South China., *Ecotox. Environ. Safety*, 191, 110229.
510 Zindler, A. W., and S. R. Hart (1986), Chemical Geodynamics, *Ann. Rev. Earth Planet. Sci.*, 14,
511 493-571.
512
513

514 **References From the Supporting Information**

515 Jackson, M., S. R. Hart, A. Koppers, H. Staudigel, J. Konter, J. Blusztajn, M. Kurz, and J. Russell
516 (2007), The return of subducted continental crust in Samoan lavas, *Nature* 448, 684-687.
517 Jackson, M. G., et al. (2020), Ancient He and W isotopic signatures preserved in mantle domains
518 least modified by crustal recycling, *PNAS*, 117, 30993-31001.
519 Macpherson, C. C., D. Hilton, J. Day, D. Lowry, and K. Gronvold (2005), High- $^3\text{He}/^4\text{He}$, depleted
520 mantle and low $d^{18}\text{O}$, recycled oceanic lithosphere in the source of central Iceland magmatism,
521 *Earth Planet. Sci. Lett.*, 233, 411-427
522 Füre, E., D. Hilton, S. Halldórsson, P. Barry, D. Hahm, T. Fischer, and K. Grönvold (2010),
523 Apparent decoupling of the He and Ne isotope systematics of the Icelandic mantle: The role of
524 He depletion, melt mixing, degassing fractionation and air interaction, *Geochim. Cosmochim.*
525 *Acta*, 74, 3307-3332.
526 Garapic, G., M. Jackson, E. Hauri, S. R. Hart, K. A. Farley, J. Blusztajn, and J. Woodhead (2015), A
527 radiogenic isotopic (He-Sr-Nd-Pb-Os) study of lavas from the Pitcairn hotspot: Implications for
528 the origin of EM-1 (enriched mantle 1), *Lithos*, 228, 1-11.
529

530 Figure Caption:

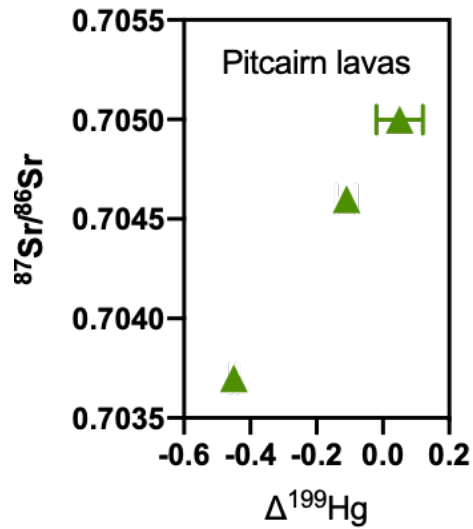
531 Figure 1: $\Delta^{199}\text{Hg}$ versus $\delta^{202}\text{Hg}$ for all samples analyzed here. Samples from the Afar, Ofu island, and Iceland have
 532 similar $\Delta^{199}\text{Hg}$ that cluster around zero and variable $\delta^{202}\text{Hg}$ values. A sample from Tubuai has a positive $\Delta^{199}\text{Hg}$
 533 value, whereas two Pitcairn samples and one Samoan sample with recycling signatures have negative $\Delta^{199}\text{Hg}$.
 534



535
 536
 537
 538
 539
 540
 541
 542
 543
 544
 545
 546
 547

548 Figure 2: $^{87}\text{Sr}/^{86}\text{Sr}$ versus $\Delta^{199}\text{Hg}$ for Pitcairn lavas. The correlation of $\Delta^{199}\text{Hg}$ values with $^{87}\text{Sr}/^{86}\text{Sr}$ suggests a
549 mixture of both recycled oceanic crust (high $^{87}\text{Sr}/^{86}\text{Sr}$ and $\Delta^{199}\text{Hg}$) and terrigenous materials (low $^{87}\text{Sr}/^{86}\text{Sr}$ and
550 $\Delta^{199}\text{Hg}$) in the Pitcairn mantle source. $^{87}\text{Sr}/^{86}\text{Sr}$ data from Garapic et al. [2015].

551



552

553

554

555

556

557

558

559

560

561

562

563

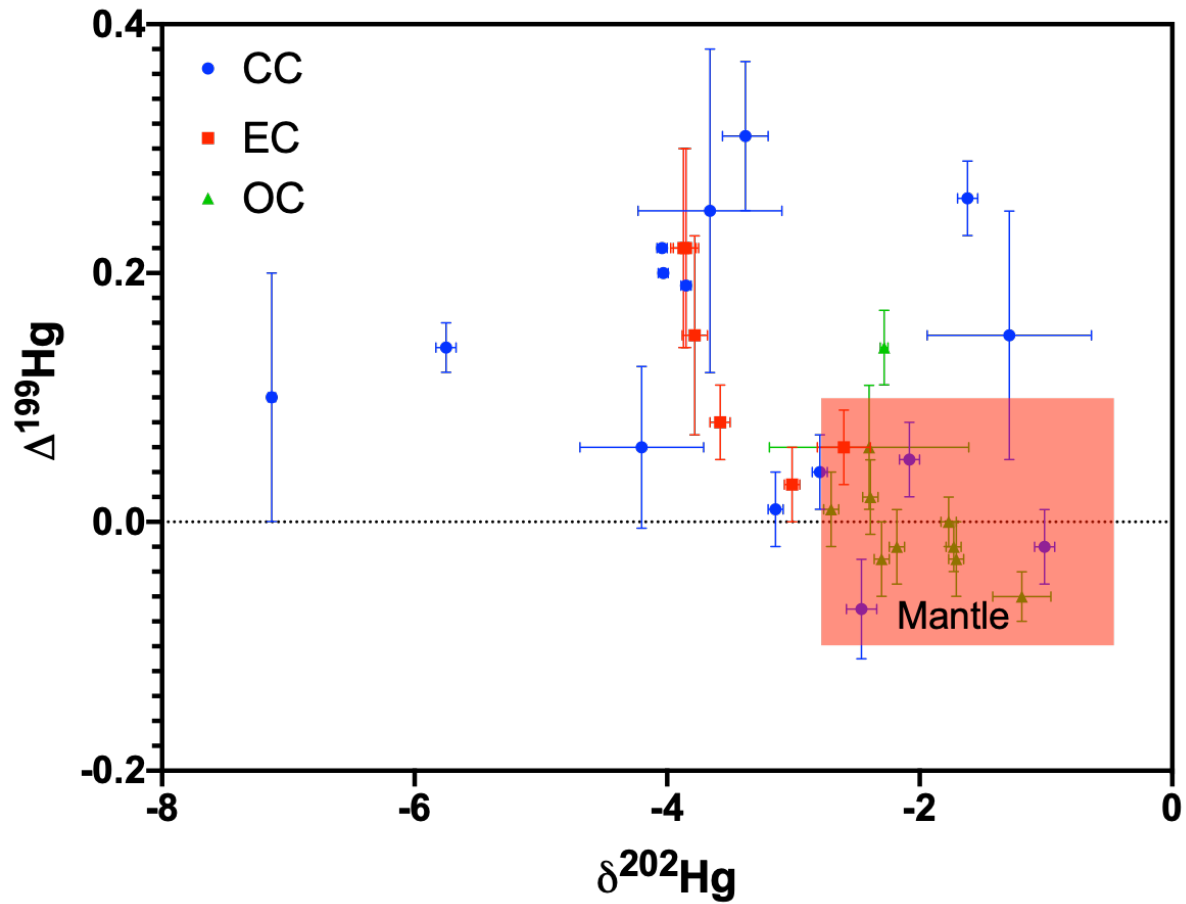
564

565

566

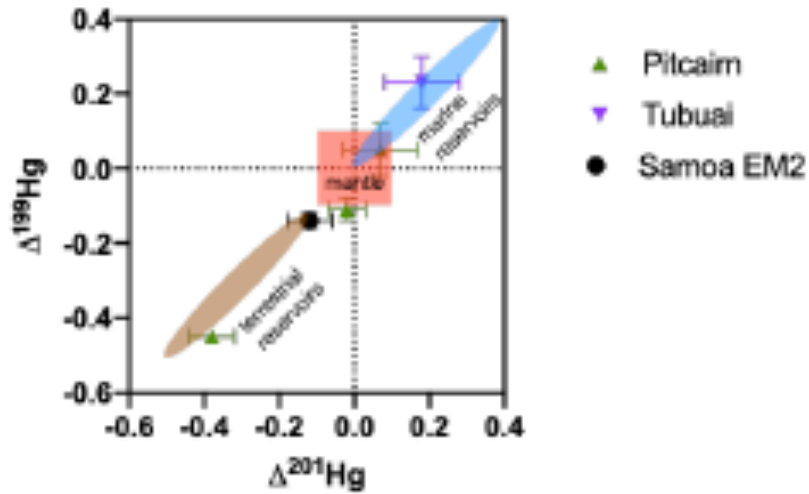
567

568 Figure 3: Mercury isotopic composition of the Earth's mantle (red box, defined by high $^3\text{He}/^4\text{He}$ lavas from Samoa
 569 and Iceland) compared to chondrites (CC=carbonaceous chondrites, EC=enstatite chondrites, OC=ordinary
 570 chondrites). Mantle-derived lavas exhibit no clear signatures for crustal recycling and fall within the chondritic
 571 range..
 572



573
 574
 575
 576
 577
 578
 579
 580

581 Figure 4: $\Delta^{199}\text{Hg}$ versus $\Delta^{201}\text{Hg}$ for the Earth's mantle (red box, defined by high $^3\text{He}/^4\text{He}$ lavas from Samoa and
 582 Iceland), Pitcairn, Tubuai and Samoa lavas. HIMU (Tubuai), EM-1 (Pitcairn) and EM-2 (Samoa) deviates from the
 583 mantle composition, reflecting a contribution of recycled surface materials in their mantle sources (marine material
 584 for Tubuai, continental material for Samoa, and both marine and continental material in the Pitcairn mantle).



585
 586
 587
 588
 589
 590
 591
 592
 593
 594
 595
 596
 597
 598
 599
 600

601 Table S1

602 **Introduction** This table contains the mercury isotopic composition the samples analysed in this study. The full data
 603 table can be found in supplementary materials (Table S1) and the Figure S1 (our Hg isotope data plotted against Nd
 604 isotope ratios). Helium isotopic data are from [Jackson *et al.*, 2007; Jackson *et al.*, 2020; Macpherson *et al.*, 2005;
 605 Furi *et al.* 2010]. All the data were collected in 2021 on a Nu Instruments Multi-collectors inductively-coupled-
 606 plasma mass-spectrometer.

607

608

609

610

611

612 **Table S1:**

613

Samples	$\delta^{202}\text{Hg}$	2SD	$\Delta^{199}\text{Hg}$	2SD	$\Delta^{200}\text{Hg}$	2SD	$\Delta^{201}\text{Hg}$	2SD	$\Delta^{204}\text{Hg}$	2SD	$^3\text{He}/^4\text{He}$ (Ra)
Afar											
AF13-339	-0.50	0.09	0.05	0.07	0.05	0.07	0.08	0.10	-0.02	0.18	
AF13-356	-1.50	0.09	0.03	0.07	0.01	0.07	-0.02	0.10	-0.07	0.18	
AF13-44	-1.09	0.09	0.05	0.07	0.03	0.07	0.05	0.10	-0.03	0.18	
AF13-48	-1.92	0.09	0.02	0.07	0.02	0.07	0.06	0.10	-0.11	0.18	
AF13-56	-1.18	0.09	-0.08	0.07	-0.07	0.07	0.01	0.10	-0.02	0.18	
AF13-90	-2.82	0.09	-0.03	0.07	0.09	0.07	0.05	0.10	-0.05	0.18	
Samoa											
ALIA-115-21	-0.55	0.03	-0.14	0.02	0.02	0.02	-0.12	0.06	-0.04	0.07	
Ofu-04-03	-2.03	0.09	-0.05	0.07	-0.02	0.07	-0.03	0.10	0.03	0.18	24
Ofu-04-06	-2.68	0.09	0.05	0.07	0.10	0.07	-0.07	0.10	-0.02	0.18	34
Ofu-04-10	-2.14	0.09	-0.04	0.07	0.01	0.07	-0.07	0.10	-0.22	0.18	22
Ofu-04-15	-1.46	0.09	-0.02	0.07	0.01	0.07	-0.03	0.10	-0.02	0.18	30
Pitcairn											
PIT-13	-1.42	0.09	0.05	0.07	0.05	0.07	0.07	0.10	0.00	0.18	9
PIT-6	-0.74	0.01	-0.45	0.01	-0.01	0.05	-0.38	0.06	0.05	0.05	
PIT-8	-0.01	0.08	-0.11	0.03	0.03	0.03	-0.02	0.05	-0.03	0.09	8
Tubuai											
TBA-B3	-3.23	0.09	0.23	0.07	0.04	0.07	0.18	0.10	-0.10	0.18	7
Iceland											
<i>Eastern Rift Zone</i>											
A11	-0.51	0.25	0.04	0.01	0.00	0.02	-0.01	0.10	0.00	0.25	24
A24	-2.07	0.10	0.01	0.13	0.03	0.08	0.01	0.10	-0.16	0.25	26
<i>Reykjanes Peninsula and Western Rift Zone</i>											
STAP-1	-1.87	0.10	-0.02	0.13	0.02	0.08	0.01	0.10	-0.01	0.25	14
VIF-1	-1.59	0.10	0.02	0.13	0.07	0.08	0.06	0.10	-0.10	0.25	13

MID-1	-1.54	0.11	0.03	0.13	0.05	0.08	0.02	0.16	0.17	0.07	17
<i>Northern Rift Zone</i>											
NAL-625	-1.93	0.02	-0.10	0.13	0.06	0.03	-0.08	0.02	0.03	0.03	34
<i>South Iceland Volcanic Zone</i>											
SAL-601	-1.14	0.10	0.06	0.13	0.06	0.08	0.01	0.10	0.04	0.25	19
Geostandards											
BCR-2	-2.18	0.09	-0.01	0.07	0.02	0.07	0.00	0.10	0.02	0.18	
BCR-2 (Geng et al.)											
	-2.08	0.08	0.00	0.14	0.01	0.08	0.00	0.14			
RGM-2	-0.98	0.09	-0.02	0.07	0.02	0.07	-0.03	0.10	0.02	0.18	
STM-2	-1.11	0.09	0.00	0.07	0.01	0.07	-0.01	0.10	-0.12	0.18	
BE-N	-3.08	0.08	0	0.03	0.01	0.03	-0.02	0.05	-0.01	0.09	
<i>Uol internal standards</i>											
I-ICE	-2.12	0.18	-0.01	0.04	0.01	0.03	-0.04	0.02	0.00	0.10	
A-ALK	-1.20	0.10	-0.03	0.13	-0.02	0.08	-0.06	0.10	0.00	0.25	
B-ALK	-2.79	0.10	0.01	0.13	0.08	0.08	-0.03	0.10	-0.01	0.25	

614
615
616
617
618
619
620
621
622
623
624
625
626
627
628
629
630
631
632

References:

- Jackson, M., S. R. Hart, A. Koppers, H. Staudigel, J. Konter, J. Blusztajn, M. Kurz, and J. Russell (2007), The return of subducted continental crust in Samoan lavas, *Nature* **448**, 684–687.
- Jackson, M. G., et al. (2020), Ancient He and W isotopic signatures preserved in mantle domains least modified by crustal recycling, *PNAS*, **117**, 30993–31001.
- Macpherson, C. C., D. Hilton, J. Day, D. Lowry, and K. Grönvold (2005), High-³He/⁴He, depleted mantle and low d¹⁸O, recycled oceanic lithosphere in the source of central Iceland magmatism, *Earth Planet. Sci. Lett.*, **233**, 411–427
- Füri, E., D. Hilton, S. Halldórsson, P. Barry, D. Hahm, T. Fischer, and K. Grönvold (2010), Apparent decoupling of the He and Ne isotope systematics of the Icelandic mantle: The role of He depletion, melt mixing, degassing fractionation and air interaction, *Geochim. Cosmochim. Acta*, **74**, 3307–3332.